UDC 532;517.4;519.6

*Issakhov A., Alpar S., Zhazylbekov N.

Faculty of Mechanics and Mathematics,
al-Farabi Kazakh National University, Almaty, Kazakhstan
*e-mail: alibek.issakhov@gmail.com

Numerical modeling of elliptic equations on unstructured and hybrid grids

Abstract. In reality, most of the physical processes are described by partial differential equations. At the same time, many application problems require numerical simulations in areas with complex geometry. Description of computational areas with complex geometric shape is best performed on unstructured and hybrid grids. An important advantage of unstructured or hybrid grid is simplicity of generation. For this purpose a large preference was given for methods that can be applied on unstructured and hybrid grids. This method is a finite volume method. One of the advantages of this discretization method is performing of local and global conservation laws, and this is very important in solving many applied problems. In the present work the variety of grids with their advantages and disadvantages are described, also the final volume method and choice of the shape of final volume are considered, discretization of the two and three dimensional Poisson equation by finite volume method is made on the unstructured and hybrid grid, formulas of finding areas, volumes and normal are described and displayed. The aim of this work is the further application of the finite volume method, and obtaining approximation of the Poisson equation in two-dimensional and three-dimensional cases on unstructured and hybrid grid. Finally, numerical results for unstructured and hybrid grids, as well as the data that obtained are compared with the analytical results, which shows good agreement. The numerical values are illustrated in the work in the form of plots.

Key words: two and three dimensional Poisson equation, unstructured mesh, hybrid mesh, finite volume method, Jacobi method.

Introduction

When we solve the fluid dynamics applications tasks one of the main problems is the computational domain. Various types of computational grids are used to describe the computational domain. Two main classes can be identified among the types of computational grids:

1. Structured mesh (regular grid).
2. Unstructured mesh (irregular grid).

Structured mesh, that shown in the Figure 1, are widely used in the field of computational fluid dynamics. When you create a regular grid, the grid nodes are an ordered structure, that have clearly defined grid direction. The main advantage of using a structured mesh is to maintain the canonical structure of the neighbors to mesh nodes. In the case of two-dimensional computational grid, cells are rectangles, and in three-dimensional case – hexagons. This type of mesh has two forms: grids with fixed (constant) step and meshes with a variable step, and the step may be constant for one of the axes and variable on other. Regular mesh allows you to use different discretization methods, in particular the finite difference method and finite volume method.Usually when you create regular grids in complex geometric areas, you need to use the coordinate transformation to build a uniform computational grid, as well as you have to write its mathematical model in curvilinear coordinates.

The main feature of unstructured grids, that shown in Figure 2, is a chaotic arrangement of mesh points in the computational domain, and as a consequence there are no areas of the grids' directions and it is impossible to arrange mesh nodes. In the three dimensional case the grid cells are used by polyhedrons and in the two dimensional case polygons with any shape. Generally, in the two dimensional case we use triangles, in the three dimensional case - tetrahedrons. The use of more complex geometric shapes is irrational in the process of meshing. Irregular mesh allows you to use different discretization methods, such as finite volume method and finite element method.

© 2016 al-Farabi Kazakh National University

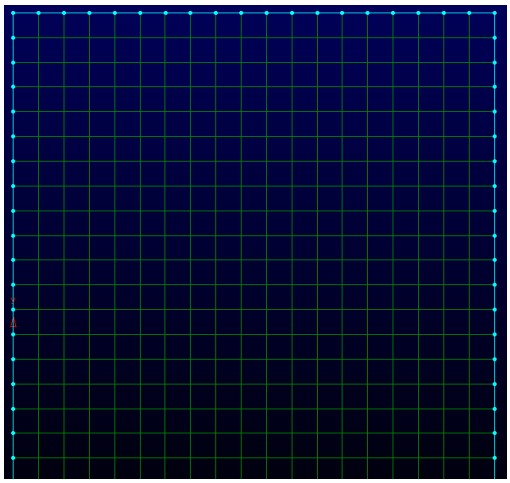

Figure 1 – Structured mesh

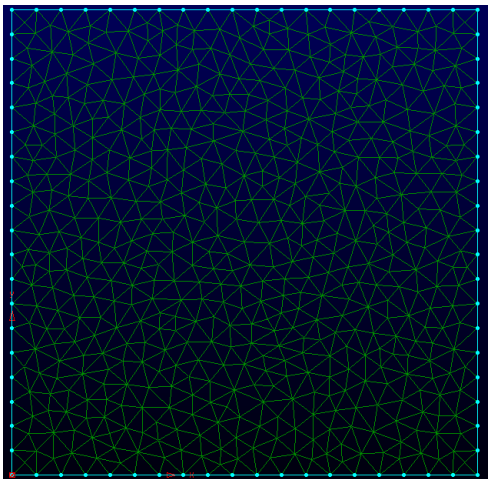

Figure 2 – Unstructured mesh

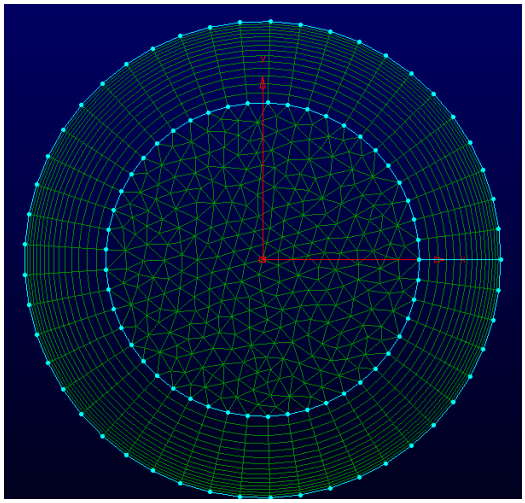

Figure 3 – Hybrid mesh

There are many ways of triangulation of calculation domain through the given points, but with any methods of triangulation we get the same number of triangles. Triangulation of the computational domain is produced according to certain criteria. One of the criterions of triangulation sounds like that – triangles, which are obtained, should be more like equilateral triangles, in other word the angles must not be too sharp. Another criterion of triangulation is triangles, that we created, shouldn't be much different in size from the neighboring triangles (mesh uniformity criterion).

The main disadvantage is the lack of data about irregular mesh structure, which leads to high costs of computing resources (computational memory). The positive features of unstructured grids are:

a) the application of this computational grids to a large number of applicable tasks;

b) minimum time in the construction of unstructured mesh as opposed to regular grids for complex geometries;

c) implementation of thickening mesh in certain areas of computational mesh by natural way.

The combination of structured and unstructured grids forms a so-called hybrid mesh (Figure 3), which allows you to take advantage from certain nets and reduce the disadvantages of a particular type of nets. Hybrid mesh often used for solving applied problems of fluid mechanics and gas mechanics.

Mathematical model

For the two variants of problems numerical solutions are compared with analytical solutions. To verify the numerical algorithm on unstructured and

hybrid meshes we used Poisson equation, which has an analytical solution. In this paper we consider two problems. In the first problem we considered a two-dimensional Poisson equation, which was solved on unstructured grids. In the second problem we considered a three-dimensional Poisson equation, which was solved on unstructured and hybrid computing meshes.

The first problem (two-dimensional equation):

$$\frac{\partial^2 u}{\partial x^2}+\frac{\partial^2 u}{\partial y^2}+3u=$$
$$=-2\sin(x+2y)+16e^{2x+3y}$$

$$u\big|_{x=0}=\sin(x+2y)+e^{2x+3y}$$
$$u\big|_{x=0.25}=\sin(x+2y)+e^{2x+3y}$$
$$u\big|_{y=0.5}=\sin(x+2y)+e^{2x+3y}$$
$$\left.\frac{\partial u}{\partial y}\right|_{y=0}=2\cos(x+2y)+3e^{2x+3y}$$

This equation has an analytic solution of this type:

$$u=\sin(x+2y)+e^{2x+3y}$$

The second problem (three-dimensional equation):

$$\frac{\partial^2 u}{\partial x^2}+\frac{\partial^2 u}{\partial y^2}+\frac{\partial^2 u}{\partial z^2}+10u=$$
$$=-4\cos(3x+y-2z)+12e^{x-z}+10$$

$$u\big|_{x=0}=\cos(3x+y-2z)+e^{x-z}+1$$
$$u\big|_{x=0.25}=\cos(3x+y-2z)+e^{x-z}+1$$
$$u\big|_{y=0}=\cos(3x+y-2z)+e^{x-z}+1$$
$$u\big|_{y=0.5}=\cos(3x+y-2z)+e^{x-z}+1$$
$$u\big|_{z=0}=\cos(3x+y-2z)+e^{x-z}+1$$
$$\left.\frac{\partial u}{\partial z}\right|_{z=0.5}=2\sin(3x+y-2z)-e^{x-z}$$

This equation has an analytic solution of this type:

$$u=\cos(3x+y-2z)+e^{(x-z)}+1$$

Approximation of the equations

Poisson's equation was approximated by using the control volume method and it was solved numerically by Jacobi method. For the application of the approximation by method of control volume we used Gauss's theorem with further replacement of the surface integral to a finite sum, that has the form:

$$\int_{V_0}\nabla\cdot(k\nabla\phi)dV=\int_S k\nabla\phi\cdot\bar{n}dA$$

Since the number of faces is limited, we can replace the surface integral sum with:

$$\int_S k\nabla\phi\cdot\bar{n}dA\approx\sum_f k_f\left(\nabla\phi\right)_f\cdot\bar{n}_f A_f=S_{\phi,0}V_0$$

The next task is to express $\left(\nabla\phi\right)_f\cdot\bar{n}_f$ through the values of the center of the cell. For this we consider the operator Nabla.

$$\nabla\phi=\left(\frac{\partial\phi}{\partial x}\bar{i}+\frac{\partial\phi}{\partial y}\bar{j}+\frac{\partial\phi}{\partial z}\bar{k}\right)$$

The above Nabla operator can be written by another basis vectors. That is for the unit normal vector, two unit tangent and to the normal vector that perpendicular to the plane.

$$\nabla\phi=\left(\frac{\partial\phi}{\partial n}\bar{n}+\frac{\partial\phi}{\partial t_1}\bar{t}_1+\frac{\partial\phi}{\partial t_2}\bar{t}_2\right)$$

Similarly, for the new base:

$$\nabla\phi=\left[\left(\nabla\phi\right)\cdot\bar{n}\right]\bar{n}+\left[\left(\nabla\phi\right)\cdot\bar{t}_1\right]\bar{t}_1+\left[\left(\nabla\phi\right)\cdot\bar{t}_2\right]\bar{t}_2$$

The two-dimensional case on the unstructured grid (Figure 4).

$$\nabla\phi=\left[\left(\nabla\phi\right)\cdot\bar{n}_f\right]\bar{n}_f+\left[\left(\nabla\phi\right)\cdot\bar{t}_f\right]\bar{t}_f$$

Lets consider the vector $\bar{l}$, that connects the two centers of the neighboring cells. Then lets perform scalar multiplication of vector $\bar{l}$ with Nabla operator.

$$(\nabla\phi)_f \cdot \bar{l} = \left[(\nabla\phi)_f \cdot \bar{n}_f\right]\delta_f + \left[(\nabla\phi)_f \cdot \bar{t}_f\right]\bar{t}_f \cdot \bar{l}$$

For approximation of $(\nabla\phi)_f \cdot \bar{l}$ to the cell centers, lets expand it in a Taylor series,and with the non-trivial action we get:

$$(\nabla\varphi)_f \cdot \bar{n}_f = \frac{\varphi_1 - \varphi_0}{\delta_f} - \frac{\left[(\nabla\varphi)_f \cdot \bar{t}_f\right]\bar{t}_f \cdot \bar{l}}{\delta_f}$$

$$J_f = \left[(\nabla\varphi)_f \cdot \bar{t}_f\right]\bar{t} \cdot \bar{l}$$

Letsconsiderseparately J_f.

$$(\nabla\phi)_f \cdot \bar{t}_f = \frac{\phi_a - \phi_b}{|\bar{t}_f|}$$

$$J_f = \left(\frac{\phi_a - \phi_b}{|\bar{t}_f|}\right)\bar{t}_f \cdot \bar{l}_f$$

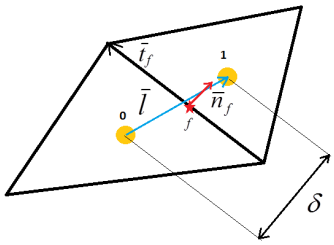

Figure 4 – Two adjacent cells of unstructured mesh

Eventually the approximation of the two-dimensional case can be written like following formula:

$$\sum_f k_f (\nabla\phi)_f \cdot \bar{n}_f A_f = \sum_f k_f \left(\frac{\phi_1 - \phi_0}{\delta_f} - \left[\frac{\phi_a - \phi_b}{\delta_f |\bar{t}_f|}\right]\bar{t}_f \cdot \bar{l}_f\right) A_f = S_{\phi,0} V_0$$

And for the three-dimensional case lets go back to the main final volume equation.

$$\sum_f k_f (\nabla\phi)_f \cdot \bar{n}_f A_f = S_{\phi,0} V_0$$

We take Nabla operator for normal and for his two orthogonal tangent vectors.

$$\nabla\phi = \left[(\nabla\phi)\cdot\bar{n}\right]\bar{n} + \left[(\nabla\phi)\cdot\bar{t}_1\right]\bar{t}_1 + \left[(\nabla\phi)\cdot\bar{t}_2\right]\bar{t}_2$$

Consider a gradient, that is shown below.

$$(\nabla\varphi)_f \cdot \bar{l} = \left[(\nabla\varphi)_f \cdot \bar{n}_f\right]\bar{n}_f \cdot \bar{l} + \left\{\left[\bar{n}_f \times (\nabla\varphi)_f\right]\times\bar{n}_f\right\}\cdot\bar{l}$$

As well as the two-dimensional case $(\nabla\phi)_f \cdot \bar{l} \approx \phi_1 - \phi_0$ and $\delta = \bar{n}\cdot\bar{l}$

$$(\nabla\varphi)_f \cdot \bar{n}_f = \frac{\varphi_1 - \varphi_0}{\delta} - \frac{\left\{\left[\bar{n}_f \times (\nabla\varphi)_f\right]\times\bar{n}_f\right\}\cdot\bar{l}}{\delta} = \frac{\varphi_1 - \varphi_0}{\delta} - \frac{J_T}{\delta}$$

where J_T – tangential flow. Let us consider now a triangular face (Figure 6), in which we try to extract J_T.

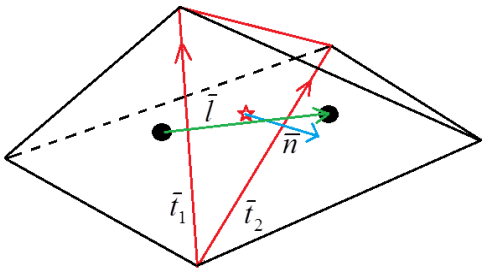

Figure 5 – Two neighboring tetrahedron

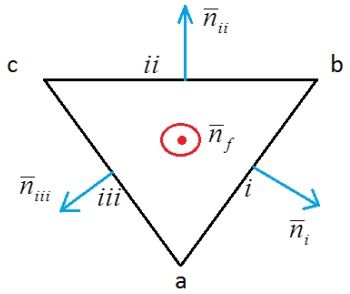

Figure 6 - The face of a tetrahedron

$$(\nabla\phi)_f = \frac{1}{A_f}\sum_{e=1}^{3}\overline{n}_e\phi_e L_e$$

Substitute it in tangential flow equation:

$$J_T = \left\{\left[\overline{n}_f \times \frac{1}{A_f}\sum_{e=1}^{3}\overline{n}_e\varphi_e L_e\right]\times\overline{n}_f\right\}\cdot\overline{l} =$$

$$= \left\{\left[\frac{1}{A_f}\sum_{e=1}^{3}\left[\left(\overline{n}_f\times\overline{n}_e\right)\times\overline{n}_f\right]\varphi_e L_e\right]\right\}\cdot\overline{l}$$

Let us use the properties of the mixed multiplication of vectors:

$$\left(\overline{b}\times\overline{c}\right)\times\overline{d} = \left(\overline{d}\cdot\overline{b}\right)\cdot\overline{c} - \left(\overline{d}\cdot\overline{c}\right)\cdot\overline{b}$$

Consequently:

$$J_T = \left\{\left[\frac{1}{A_f}\sum_{e=1}^{3}\left[\left(\overline{n}_f\cdot\overline{n}_f\right)\overline{n}_e - \left(\overline{n}_f\cdot\overline{n}_e\right)\overline{n}_f\right]\varphi_e L_e\right]\right\}\cdot\overline{l} =$$

$$= \left\{\left[\frac{1}{A_f}\sum_{e=1}^{3}\overline{n}_e\varphi_e L_e\right]\right\}\cdot\overline{l}$$

During non-trivial transformations we obtain our final approximation of the Helmholtz equation for two-dimensional and three-dimensional case. The problem is solved iteratively by using the Jacobi method.

Final form of discrete Jacobi method by using unstructured mesh for two-dimensional Poisson equation will look like this equation:

One of the problems when we calculate J_T is the normal $(\overline{n}_e)$ to the side of faces of the finite volume element.

$$\overline{n}_e = \overline{t}_e \times \overline{n}_f$$

Substitute $\overline{n}_e$ in J_T, weget:

$$J_T = \frac{1}{A_f}\sum_{e=1}^{3}\phi_e\left(\left[L_e\overline{t}_e\times\overline{n}_f\right]\cdot\overline{l}\right)$$

When we multiply the length of the side L_e to the unit vector $\overline{t}_e$ that will become equal to the vector $\overline{T}_e$, which describes the whole side faces.

$$\overline{T}_e = L_e\overline{t}_e$$

Then we use properties of the mixed multiplication of vectors and apply it for the above mentioned equation.

$$J_T = \frac{1}{A_f}\sum_{e=1}^{3}\phi_e\left(\overline{T}_e\cdot\left[\overline{n}_f\times\overline{l}\right]\right)$$

Returning to the expression $(\nabla\varphi)_f\cdot\overline{n}_f$ lets substitute, that we found in J_T:

$$(\nabla\phi)_f\cdot\overline{n}_f = \frac{\phi_1-\phi_0}{\delta} - \frac{1}{\delta A_f}\left(\sum_{e=1}^{3}\phi_e T_e\right)\cdot\left[\overline{n}_f\times\overline{l}\right]$$

$$\sum_f k_f\left\{\frac{\phi_{nb(f)}-\phi_0}{\delta_f} - \frac{1}{\delta_f A_f}\sum_{e=1}^{n_{e(f)}}\phi_e\left(\overline{T}_e\cdot\left[\overline{n}_f\times\overline{l}_f\right]\right)\right\}A_f = S_{\phi,0}V_0$$

$$u_i^{n+1} = \frac{\left(\sum_f\left(\frac{u^n_{i,nb(f)}}{\delta_{i,f}} - \left[\frac{u^n_{i,a(f)}-u^n_{i,b(f)}}{\delta_{i,f}\left|\overline{t}_{i,f}\right|}\right]\overline{t}_{i,f}\cdot\overline{l}_{i,f}\right)A_{i,f}\right)}{\left(\sum_f\frac{A_{i,f}}{\delta_{i,f}} - 3V_i\right)} -$$

$$-\frac{\left(-2\sin(x+2y)+16e^{2x+3y}\right)V_i}{\left(\sum_f\frac{A_{i,f}}{\delta_{i,f}} - 3V_i\right)}$$

Final discrete form of Jacobi method by using unstructured mesh for two-dimensional Poisson equation will look like this:

$$u_i^{n+1} = \frac{\left(\sum_f \left(\frac{u_{i,nb(f)}^n}{\delta_{i,f}} - \frac{1}{\delta_{i,f} A_{i,f}} \left(\sum_{e=1}^{3} u_{i,f,e}^n \bar{t}_{i,f,e}\right) \cdot \left[\bar{n}_{i,f} \times \bar{l}_{i,f}\right]\right) A_{i,f}\right)}{\left(\sum_f \frac{A_{i,f}}{\delta_{i,f}} - 10V_i\right)} -$$

$$- \frac{\left(-4\cos(3x + y - 2z) + 12e^{x-z} + 10\right)V_i}{\left(\sum_f \frac{A_{i,f}}{\delta_{i,f}} - 10V_i\right)}$$

Results of numerical calculations

In the first problem for the two-dimensional Poisson equation physical area is used with the sizes Lx = 0.25 and Ly = 0.5, which is approximated by using triangles. The number of physical computing points 1471, number of cells 2764. As shown in Figure 7, computational grid is stressed at the point (0.25, 0.5), because in this area the Neumann boundary condition is used and to minimize the numerical errors we had to stress the computational grid at the given point. For the second problem for the three-dimensional Poisson equation physical area is used with the sizes Lx = 0.25, Ly = 0.5, Lz = 0.5, which is approximated by using tetrahedrons for the unstructured mesh. Number of nodes 4687, number of cells 23084. (Figure 8).

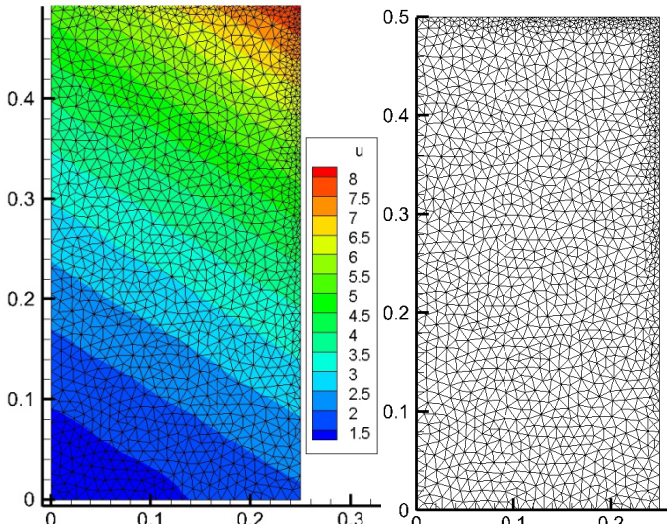

Figure 7 – A two-dimensional grid with numerical solution. The maximum error is equal to 0.0654(0.7%).

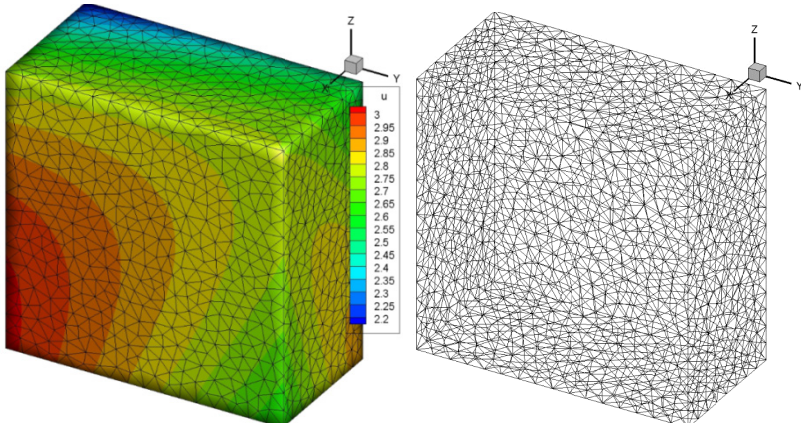

Figure 8 – Three-dimensional mesh with the numerical solution. The maximum error is equal to 0.026(0.9%).

To reduce the numerical errors for unstructured meshes the hybrid mesh was used. For a hybrid three-dimensional problem the conditions of the second problem are used (three-dimensional Puassson equation). For this purpose computing region is divided into two blocks: unstructured and structured meshes, which will consist of tetrahedrons, hexagons and pyramids. Number of points 1812, number of cells 4380. Grid stressed along Z axis to the face, where the Neumann boundary condition is defined (fig.9). The following figures show benefits of unstructured and hybrid meshes on objects with various shapes.

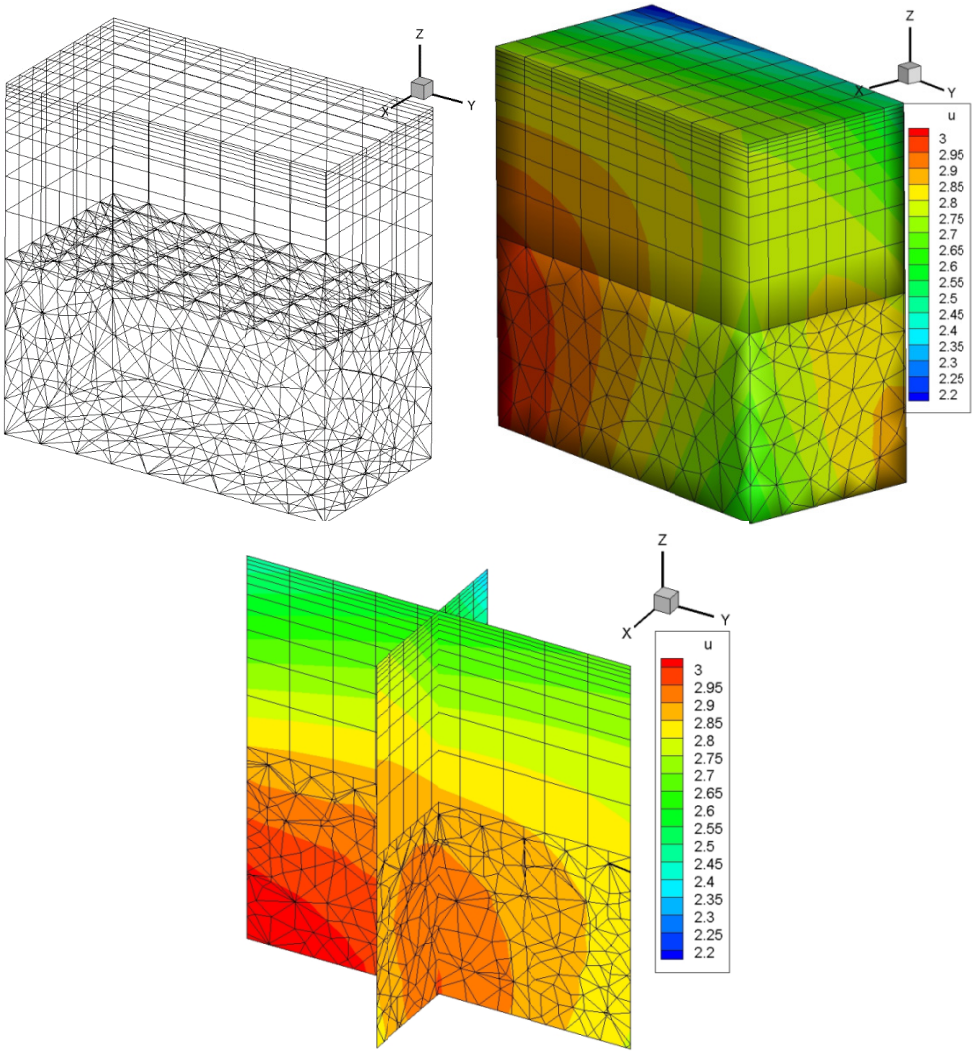

Figure 9 - The hybrid mesh with the numerical solution.
The maximum error is equal to 0.0114(0.4%).

Conclusion

During implementation of this work on the basis of numerical solution of two-dimensional and three-dimensional Poisson equations, test computations of finite volume method on unstructured grids were made. And also an analysis of solutions was performed for the three-dimensional Poisson equation using a hybrid mesh.

When we compared the results of numerical results of three-dimensional Poisson equation for unstructured and hybrid meshes, it may be noted that the numerical error is reduced when we use the hybrid mesh, and also computing resources used much less.

As a result of our investigation, according to the data that obtained, it can be said that the regular computational grid has the advantage in the

accuracy of the solution, but by adapting unstructured computational mesh to complex geometry wa can create hybrid mesh, which will compensate the pros and cons of structured and unstructured grids..

In the paper it is shown that by using unstructured mesh numerical error equal 0.9%, and using a hybrid grid numerical error does not exceed 0.4%. From this we can conclude that it is necessary to use a structured grid in the area where it is possible and necessary to use unstructured grid where we can not use a structured grid.

References

1. Mazumder S. -Numerical methods for partial differential equation: Finite Difference and Finite Volume Methods. – Academic Press, 2015. – 484 p.

2. Versteeg H.K. Malalasek Introduction to computational fluid dynamics The finite volume method. – Pearson, 2007. – 520p.

3. F.Moukalled L.Mangani M.Darwish - The finite volume method in computational fluid dynamics. – Springer, 2015. –791p.

4. Fletcher K. Vychislitel'nye metody v dinamike zhidkostej. – Moscow: Mir, 1991. –Vol.2. – 552 p.

5. Chung T.J. Computational fluid dynamics. – Cambridge University Press, 2002. –1012 p.

6. Anderson D., Tannehil Dzh., Fletcher R. - Vychislitel'naja gidromehanika i teploobmen. Moskva, Mir, 1990. –Vol. 2. – 392 p.

7. Issakhov A., Mathematical modeling of the discharged heat water effect on the aquatic environment from thermal power plant // International Journal of Nonlinear Science and Numerical Simulation, – 2015. – Vol.16, No 5. – P. 229–238, doi:10.1515/ijnsns-2015-0047.

8. Issakhov A., Mathematical modeling of the discharged heat water effect on the aquatic environment from thermal power plant under various operational capacities // Applied Mathematical Modelling. – 2016. – Vol. 40, No 2. – P. 1082–1096

9. Issakhov A. Large eddy simulation of turbulent mixing by using 3D decomposition method // J. Phys.: Conf. Ser. – 2011. –Vol.318, No 4. –P. 1282-1288.

10. Ferziger J.H., M. Peric - Computational Methods for Fluid Dynamics. – Springer, 2013. – 440 p.

11. Firsov D.K. Metod kontrol'nogo ob'ema na nestrukturirovannoj setke v vychislitel'noj matematike. – Tomsk, 2007. – 72 p.